HHS Public Access

Author manuscript

*J Am Chem Soc*. Author manuscript; available in PMC 2016 June 10.

Published in final edited form as:

*J Am Chem Soc*. 2015 June 10; 137(22): 7145–7151. doi:10.1021/jacs.5b02383.

# CalFluors: A Universal Motif for Fluorogenic Azide Probes across the Visible Spectrum

**Peyton Shieh**[†], **Vivian T. Dien**[†], **Brendan J. Beahm**[†], **Joseph M. Castellano**[‖], **Tony Wyss-Coray**[‖], and **Carolyn R. Bertozzi**[†,‡,§,*]

[†]Department of Chemistry, University of California, Berkeley, California 94720, United States

[‡]Department of Molecular and Cell Biology, University of California, Berkeley, California 94720, United States

[§]Howard Hughes Medical Institute, University of California, Berkeley, California 94720, United States

[‖]Department of Neurology and Neurological Sciences, Stanford University School of Medicine, Stanford, California 94305, United States

## Abstract

Fluorescent bioorthogonal smart probes across the visible spectrum will enable sensitive visualization of metabolically labeled molecules in biological systems. Here we present a unified design, based on the principle of photoinduced electron transfer, to access a panel of highly fluorogenic azide probes that are activated by conversion to the corresponding triazoles via click chemistry. Termed the CalFluors, these probes possess emission maxima that range from green to far red wavelengths, and enable sensitive biomolecule detection under no-wash conditions. We used the CalFluor probes to image various alkyne-labeled biomolecules (glycans, DNA, RNA, and proteins) in cells, developing zebrafish, and mouse brain tissue slices.

## Graphical abstract

[*]**Corresponding Author**. crb@berkeley.edu.

**ASSOCIATED CONTENT**

Supporting Information

Supplementary figures, synthetic procedures, and experimental protocols. The Supporting Information is available free of charge on the ACS Publications website at DOI: 10.1021/jacs.5b02383.

The authors declare no competing financial interest.

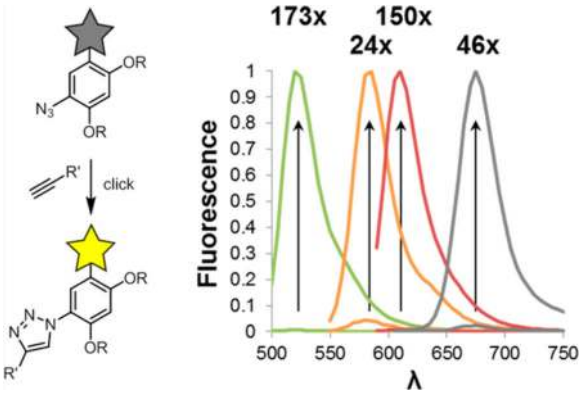


## INTRODUCTION

Bioorthogonal smart probes enable the detection of labeled biomolecules in settings where it is difficult to remove excess probe.[1,2] In a typical embodiment, the bonding changes accompanying the bioorthogonal reaction lead to unquenching of a latent fluorophore. As an example, we recently reported the design of fluorogenic azide probes that are activated by Cucatalyzed or metal-free click chemistry with alkyne-labeled biomolecules.[3,4] Building from the elegant work of Nagano and co-workers,[5] we designed these molecules to be internally quenched via photoinduced electron transfer (PeT) in the azide-functionalized form, and unquenched upon conversion of the azide to a triazole (Figure 1A).

Key to these efforts was the identification of a pendent aryl ring system that imparts the desired electronic effects on a given fluorophore scaffold. Using computational methods, we first arrived at the azidonaphthyl group of fluorescein analogue **1** (Figure 1B), which afforded a 30-fold fluorescence enhancement upon triazole formation.[3] However, the azidonaphthyl "switch" was considerably less effective in other fluorophore structures. Instead, a Si-rhodamine analogue was more potently quenched by a pendent 3-azido 4,6-dimethoxybenzene moiety (compound **2**, Figure 1B).[4] Indeed, this switching group afforded a 5-fold higher fluorescence response than any other aryl system screened.

In an effort to accelerate the design of activatable azide probes with various photophysical and photochemical properties, we sought to identify a universal switch capable of PeT across a variety of dye structures. Here we report that the 3-azido 4,6-dialkoxyaryl group possesses this capability. Incorporation of this group into various xanthene scaffolds afforded a palette of dyes that emit at green to far red wavelengths. When functionalized with zwitterionic solubilizing groups, these probes enabled robust and sensitive detection of alkyne-labeled biomolecules under no-wash conditions and in a variety of settings, including live cells and tissue sections. We call the probes *C*lick *A*ctivated *L*uminogenic Fluorophores, or Cal-Fluors.

## RESULTS AND DISCUSSION

In our recent study, we identified the 3-azido-4,6-dimethoxybenzene substituent as a fluorogenic switch that outperformed many other aryl substituents examined.[4] To further

understand the electronic basis of this superior performance, we synthesized a panel of azide- and triazole-functionalized aryl rings (**3–7**, Figure 2A) and determined their oxidation potentials using cyclic voltammetry (Figure 2B). The measured oxidation potentials reflect the compounds' propensity to donate an electron, which would result in fluorescence quenching via PeT. Consistent with calculations, we found that all the triazoles had higher oxidation potentials than their parent azides (Figure 2C). Among the aryl azides, compound **3a** was the most electron rich, underscoring its potent quenching activity, and its change in oxidation potential upon conversion to triazole **3b** was the most dramatic (Figure 2C). This large change is consistent with computational predictions that an *ortho*-substituent forces the triazole to twist further out of plane and prevents donation from the nitrogen lone pair into the aryl system (Figure S1). We found that calculated $E_{HOMO}$ and oxidation potential correlate (Figure S2), though the modest fit suggests that more sophisticated approaches toward predicting PeT efficiency may be necessary for future improvements in computation-based probe design. Nevertheless, these results gave us confidence that dimethoxy aryl ring **3** would efficiently switch fluorescence in a variety of fluorophore systems, regardless of subtle differences in their electronics.

To test this hypothesis, we expanded our panel of xanthene fluorophores containing the 3-azido 2,4-dimethoxybenzene substituent. We focused on fluorescein, tetramethylrhodamine (rhodamine), and dimethylsilicon-substituted fluorescein (Si-fluorescein)[6] scaffolds, which have emission maxima of around 520 nm (green, compound **8**), 580 nm (orange, compound **9**), and 610 nm (red, compound **10**), respectively (Figure 3A). Following a general route, 3-bromo-4,6-dimethoxy aniline was protected, lithiated, and then added into various protected xanthones to generate the corresponding amino-fluorescein, -rhodamine, and -Si-fluorescein derivatives (Scheme S1). While the fluorescein and Si-fluorescein xanthones were readily prepared via literature procedures,[3,6] we developed a new route to access the rhodamine xanthone from commercially available Pyronin Y (see Supporting Information). These amine-functionalized probes were converted to aryl azides by diazotization and displacement with sodium azide to generate compounds **8a–10a**. The corresponding triazoles, **8b–10b**, were prepared under Cu-catalyzed click conditions.

The fluorescence quantum yields of the azides and triazole products were measured in pH 7.4 phosphate-buffered saline. Gratifyingly, we found that their common dimethoxy aryl substituent efficiently switched fluorescence for all fluorophores tested (Table 1). Notably, the fluorescein and Si-fluorescein probes offered higher levels of fluorescence enhancement than any of our previously reported fluorogenic azide probes. In particular, Si-fluorescein **10a**, which has an emission maximum beyond 600 nm, underwent >100-fold enhancement in fluorescence upon click reaction. Rhodamine **9a**, however, showed a significantly lower turn-on ratio (20-fold) due to reduced quenching of the azide starting material. All of the probes were good substrates for the Cu-catalyzed click reaction,[7] achieving complete conversion to the corresponding triazoles within 10 min using micromolar concentrations of catalyst and reagents (Figure S3).

A significant advantage of these probes is that, by replacing the methoxy groups with other alkyloxy functionalities, their physical properties can be altered without perturbing the electronics of the system. In previous work, we found that introducing oligoethylene glycol

tails significantly improved the water solubility of our probes while maintaining fluorescence enhancement.[4] We synthesized the bis-oligoethylene glycol functionalized azidofluorescein derivative **11a** as well as its triazole derivative **11b** (Figure 3B, Scheme S2). This fluorescein analogue maintained the enhancement in fluorescence of the parent fluorophore while showing good water solubility, making it very well-suited for biological labeling experiments (Table 1, also see Supporting Information).

The robustness of this route enabled us to access oligoethylene glycol functionalized rhodamine and Si-fluorescein probes as well, however we found their aqueous solubility to be limiting for biological labeling purposes. We were concerned that potential for nonspecific protein binding would lead to spurious fluorescence turn-on, as documented by Nagano and co-workers in other systems.[8] While were able to improve water solubility of the Si-rhodamine derivative by adding sulfate esters at the termini of oligoethylene glycol chains, but this compound was still subject to fluorescence enhancements due to protein and lipid binding (Figure S4). As well, selective sulfation would have been difficult to achieve for fluorescein-based probes that possess competing phenolic hydroxyl groups.

In a search for alternative solubilizing groups, we were drawn to zwitterions, which are growing in popularity as anti-fouling agents in biomaterials applications.[9] Indeed, zwitterionic coatings have been shown to outperform polyethylene glycols in many situations.[10–12] Additionally, zwitterionic fluorophores have been recently demonstrated to have dramatically reduced serum binding compared to anionic counterparts.[13] To generate fluorophores containing zwitterionic tails, we were drawn to the sulfo-betaine scaffold, which can be generated by the reaction of tertiary amines with 1,3-propanesultone.[14] The mild reaction conditions suggested that these functionalities could be introduced at the end of our synthetic route, thereby minimizing difficulties in product isolation. Accordingly, we prepared a panel of zwitterionic azide fluorophores according to the route shown in Scheme S3. In keeping with tradition in this field, we have given the azide fluorophore products the common names CalFluor 488, 555, 580, and 647, respectively (wherein the numbers represent recommended excitation wavelengths) (Figure 4A).

All the CalFluors underwent significant fluorescence enhancement upon triazole formation at a level that was at least as high as their dimethoxy substituted counterparts (Figure 4B, Table 1). CalFluor 488 and 580 showed higher levels of fluorescence enhancement compared to their parent derivatives, potentially due to subtle electronic differences conferred by the oligoethylene glycol tails. Additionally, the fluorescence of these probes remained virtually unaltered in proteinaceous environments (e.g., 3% BSA or neat fetal bovine serum, Figure S5) or in the presence of detergents such as Triton X-100 and Tween-20 (Figure S6), demonstrating how effectively these zwitterionic tails minimize non-specific interactions.

Our next goal was to evaluate the CalFluors' performance in no-wash cell imaging experiments. Using established methods, we metabolically labeled cell-surface glycoconjugates with peracetylated *N*-pentynoyl mannosamine ($Ac_4$ManNAl), which introduces terminal alkyne groups into sialic acid residues (SiaNAl).[15,16] HEK 293T cells treated in this fashion were then incubated, without fixation, with a cocktail containing 50

μM $CuSO_4$, 300 μM BTTAA, 5 mM sodium ascorbate, and 10 μM CalFluor dye.[7] After 15 min, cell surface glycans were robustly labeled with the given fluorophore, whereas control cells treated with peracetylated *N*-acetylmannosamine ($Ac_4$ManNAc) showed no detectable fluorescence (Figure 5A). The only background fluorescence was from free fluorophore in solution (Figure S7, only observable at high contrast). Similar results were achieved with CHO K1 cells (Figure S8). Labeling with CalFluor probes could be observed in real time, and clear fluorescence over background was visible just minutes into the reaction (Figure S9). Notably, under the same reaction conditions, CalFluors labeled cells far more intensely than the blue fluorogenic probe 3-azido-7-hydroxycoumarin (Figure S10),[17] which we attribute in part to the CalFluors' superior reactivity (Figure S11). This observation is consistent with studies by Finn and co-workers showing that electron-rich aryl azides undergo more rapid copper-catalyzed click reactions.[18]

We also evaluated fixed (3% paraformaldehyde) $Ac_4$ManNAltreated HEK 293T cells as substrates CalFluor labeling. In this case, copper-click reaction with 50 μM $CuSO_4$ and 300 μM BTTAA gave poor labeling, potentially due to sequestration of the copper catalyst by denatured proteins. However, use of higher catalyst concentrations (100 μM TBTA, 1 mM $CuSO_4$, 2 mM sodium ascorbate) gave robust labeling with 10 μM CalFluor dyes (Figure 5B). While some background was apparent when using CalFluor 555 at this concentration, a single wash step was sufficient to eliminate this background fluorescence (Figure S12). Similar results were achieved when performing the same experiments on fixed CHO K1 cells (Figures S13 and S14).

Under these copper-click conditions, the 3-azido-7-hydroxycoumarin probe performed comparably to the CalFluors when labeling fixed cells (Figure S15). By contrast, the sulfated predecessor **S1** or the oligoethylene glycol containing probe **11** gave higher background fluorescence, underscoring the benefit of the zwitterionic tails in reducing non-specific interactions. (Figures S16 and S17). The advantage of the fluorescence turnon of CalFluors was clear when comparing labeling by the nonfluorogenic AlexaFluor 647 alkyl azide. (Figure S18). Even with a washing step, background from unreacted fluorophore obscured any alkyne-dependent signal.

We next tested our probes for visualization of glycans *in vivo*. Zebrafish have been powerful model system for the study of development using optical methods due to their optical transparency. Our laboratory has had a longstanding interest in imaging glycans during zebrafish development.[19–23] To test the utility of CalFluors in this system for such applications, we injected zebrafish embryos at the single-cell stage with SiaNAl.[20] After either 24 or 36 h post-fertilization (hpf), the embryos were bathed in a solution containing a CalFluor probe along with copper catalyst. We observed bright alkynedependent fluorescence on cells of the enveloping layer without washing (Figure 6A). Fluorescence signal increased over time and maximized after 20 min. Importantly, in similar labeling experiments performed with the non-fluorogenic AlexaFluor 594 alkyl azide probe or the blue-emitting 3-azido-7-hydroxycoumarin (Figure 6B), high levels of background fluorescence from unreacted probe or endogenous biomolecules, respectively, obscured alkyne-dependent labeling.

Beyond glycans, the small size of linear alkynes has enabled its incorporation into a wide variety of intracellular biomolecules. For example, linear alkynes have been used to label newly synthesized DNA and RNA via 5-ethynyl deoxyuridine (EdU) and 5-ethynyl uridine (EU), respectively. In particular, this click-chemistry based approach to visualizing newly synthesized DNA/RNA remains superior to related methods such as BrdU labeling as a harsh denaturation step is not necessary.[24–27] Additionally, linear alkynes can be incorporated into newly synthesized proteins by the incorporation of homopropargylglycine (HPG) in methionine-starved cells.[28–31]

We first tested the suitability of our probes for imaging EdUlabeled DNA. We treated HEK 293T cells with 10 μM EdU for 12 h, fixed and permeabilized the cells, and then labeled them with our azide probes under copper-click conditions. We hoped that the use of fluorogenic azide probes for EdU detection would streamline the visualization of newly synthesized DNA. Gratifyingly, we saw robust labeling using all four of our probes without the need to wash away excess reagent (Figure 7A,B). Results were significantly better than those achieved using other azide fluorophores under similar labeling conditions. (Figures 7B, S19, and S20). We noticed that the fluorescein-based probes (CalFluors 488 and 580) labeled intracellular DNA more weakly than the related rhodamine-based probes (CalFluors 555 and 647, Figure 6B). Similar results were achieved when we labeled newly synthesized RNA by treatment of cells with 1 mM EU (Figures S21–S23). This difference may be due to the pH sensitivity of our fluorescein-based dyes, especially when conjugated to the anionic oligonucleotides (Figures S24, and S25).[32]

Importantly, our palette of probes enabled two-color imaging with other well established probes, such as with cells prelabeled with the blue-emitting Hoescht 33342 nuclear stain (Figure 7C). No-wash labeling was also suitable for CHO K1 cells labeled with EdU and EU under identical conditions, although specific signal was lower for all probes tested, likely due to poorer alkyne incorporation (Figures S26–S28). Beyond imaging mammalian cells in culture, EdU has also been used to label newly synthesized DNA in bacteria.[33] *E. coli* were grown in the presence of EdU, fixed, permeabilized, and labeled with CalFluor 647; robust alkyne-dependent labeling was observed by flow cytometry, and significantly higher signal over background was achieved compared to AlexaFluor 647 alkyl azide (Figure S29). One of the more exciting applications of EdU labeling is to visualize actively proliferating cells *in vivo*. Tissue slices were obtained from the subventricular zone of mice injected with 150 mg/kg EdU 2 h before perfusion. Gratifyingly, CalFluor 647 were able to efficiently visualize EdU from these tissue sections with excellent signal over background (Figure 7D). Finally, all four CalFluor probes were suitable for the robust detection of newly synthesized proteins containing HPG (Figure S30).

## CONCLUSION

Here, we report a general platform to generate fluorogenic azide probes across the visible spectrum. Our experiments clearly demonstrate the broad applicability of these optimized probes for labeling a large panel of alkyne-functionalized biomolecules in both live and fixed cells, in tissue, and *in vivo*. Given the generality of PeT, we anticipate that this biszwitterionic dialkoxy aryl azide motif will switch fluorescence in a wide variety of

fluorophores beyond the xanthenes. For example, other fluorophore scaffolds, such as BODIPY, cyanines, and pyrazolines, can all be efficiently switched via PeT.[34–36]

Consistent with this prediction, a recent report from Wong and co-workers demonstrated that the BODIPY scaffold can also be used as a platform for PeT-based fluorogenic azide probes.[37] Beyond developing probes with higher photostability, using our optimized aryl ring in conjunction with cyanine probes or modified Si-rhodamine probes may push emission maxima into the near-infrared.[38] PeT has also been used to modulate other properties besides fluorescence, such as the rate of singlet oxygen generation or luminescence from metal complexes.[39,40] We note that this transportable design element is reminiscent of the 1,2-diaminobenzene-based trigger for nitric oxide sensing that has been integrated into myriad dye scaffolds.[41–44] In addition, the incorporation of zwitterionic sulfobetaine tails, which significantly outperformed both oligoethylene glycol or sulfated modifications in our hands, may be a general strategy for increasing the performance of PeT-based probes in complex environments.[45] These modifications prevent probe access to the interior of living cells, but the cytotoxicity of copper catalysts likewise limits reactions with linear alkyne-functionalized biomolecules to fixed samples or the live cell surface. Future work to overcome these shortcomings may benefit from the modularity of our synthetic route toward a wide variety of fluorogenic azide probes. Beyond the applications described here, CalFluor probes may find use in visualizing linear alkyne-tagged biomolecules in large tissue samples, where reagents are difficult to wash out.[46]

Nonetheless, this current work, in combination with the established 3-azido-7-hydroxycoumarin probe, completes the panel of fluorogenic azide probes with emission maxima across the visible spectrum. With recent advances in increasing the efficiency of Cu-catalyzed click reactions, these technologies will further enhance the ease and sensitivity of detecting linear alkyne-functionalized biomolecules in biological systems.[47–49]

## Supplementary Material

Refer to Web version on PubMed Central for supplementary material.

## ACKNOWLEDGMENTS

This work was funded by NIH grants GM058867 and AI051622 to C.R.B. We thank Prof. C. Chang (UC Berkeley) for the generous use of his potentiostat and Rachelle J. Abbey (Stanford) for assistance with mouse experiments.

## REFERENCES

1. For recent reviews on bioorthogonal chemistry, see: Patterson DM, Nazarova LA, Prescher JA. ACS Chem. Biol. 2014; 9:592–605. [PubMed: 24437719] Lang K, Chin JW. ACS Chem. Biol. 2014; 9:16–20. [PubMed: 24432752] Lang K, Chin JW. Chem. Rev. 2014; 114:4764–4806. [PubMed: 24655057] Ramil CP, Lin Q. Chem. Commun. 2013; 49:11007–11022. Debets MF, van Hest JCM, Rutjes FPJT. Org. Biomol. Chem. 2013; 11:6439–6455. [PubMed: 23969529] McKay CS, Finn MG. Chem. Biol. 2014; 21:1075–1101. [PubMed: 25237856]
2. For a review on probes activated by biorthogonal reactions, see Shieh P, Bertozzi CR. Org. Biomol. Chem. 2014; 12:9307–9320. [PubMed: 25315039]
3. Shieh P, Hangauer MJ, Bertozzi CR. J. Am. Chem. Soc. 2012; 134:17428–17431. [PubMed: 23025473]

4. Shieh P, Siegrist MS, Cullen AJ. Proc. Natl. Acad. Sci. U.S.A. 2014; 111:5456–5461. [PubMed: 24706769]
5. Urano Y, Kamiya M, Kanda K, Ueno T, Hirose K, Nagano T. J. Am. Chem. Soc. 2005; 127:4888–4894. [PubMed: 15796553]
6. Egawa T, Koide Y, Hanaoka K, Komatsu T, Terai T, Nagano T. Chem. Commun. 2011; 47:4162–4164.
7. Besanceney-Webler C, Jiang H, Zheng T, Feng L, Soriano del Amo D, Wang W, Klivansky LM, Marlow FL, Liu Y, Wu P. Angew. Chem. Int. Ed. 2011; 50:8051–8056.
8. Sunahara H, Urano Y, Kojima H, Nagano T. J. Am. Chem. Soc. 2007; 129:5597–5604. [PubMed: 17425310]
9. For selected references, see: Butun V, Bennett CE, Vamvakaki M, Lowe AB, Billingham NC, Armes SP. J. Mater. Chem. 1997; 7:1693–1695. Homlin RE, Chen X, Chapman RG, Takayama S, Whitesides GM. Langmuir. 2001; 17:2841–2850. Zhang Z, Chao T, Chen S, Jiang S. Langmuir. 2006; 22:10072–10077. [PubMed: 17107002] Yang R, Xu J, Ozaydin-Ince G, Wong SY, Gleason KK. Chem. Mater. 2011; 23:1263–1272.
10. Jiang SY, Cao ZQ. Adv. Mater. 2010; 22:920–932. [PubMed: 20217815]
11. Zhang L, Cao Z, Bai T, Carr L, Ella-Menye J-R, Irvin C, Ratner BD, Jiang S. Nat. Biotechnol. 2012; 31:553–556. [PubMed: 23666011]
12. Smith RS, Zhang Z, Bouchard M, Li J, Lapp HS, Brotske GR, Lucchino DL, Weaver D, Roth LA, Coury A, Biggerstaff J, Sukavaneshvar S, Langer R, Loose C. Sci. Transl. Med. 2012; 4 No. 153ra132.
13. Choi HS, Nasr K, Alyabyev S, Feith D, Lee JH, Kim SH, Ashitate Y, Hyun H, Patonay G, Strekowski L, Henary M, Frangioni JV. Angew. Chem. Int. Ed. 2011; 50:6258–6263.
14. Huang J, Xu WJ. Appl. Polym. Sci. 2011; 122:1251–1257.
15. Hsu T-L, Hanson SR, Kishikawa K, Wang S-K, Sawa M, Wong C-H. Proc. Natl. Acad. Sci. U.S.A. 2007; 104:2614–2619. [PubMed: 17296930]
16. Chang PV, Chen X, Smyrniotis C, Xenakis A, Hu TS, Bertozzi CR, Wu P. Angew. Chem. Int. Ed. 2009; 48:4030–4033.
17. Sivakumar K, Xie F, Cash BM, Long S, Barnhill HN, Wang Q. Org. Lett. 2004; 6:4603–4606. [PubMed: 15548086]
18. Rodionov VO, Presolski SI, Diaz DD, Fokin VV, Finn MG. J. Am. Chem. Soc. 2007; 129:12705–12712. [PubMed: 17914817]
19. Laughlin ST, Baskin JM, Amacher SL, Bertozzi CR. Science. 2008; 320:664–667. [PubMed: 18451302]
20. Baskin JM, Dehnert KW, Laughlin ST, Amacher SL, Bertozzi CR. Proc. Natl. Acad. Sci. U.S.A. 2010; 107:10360–10365. [PubMed: 20489181]
21. Dehnert KW, Beahm BJ, Huynh TT, Baskin JM, Laughlin ST, Wang W, Wu P, Amacher SL, Bertozzi CR. ACS Chem. Biol. 2011; 6:547–552. [PubMed: 21425872]
22. Dehnert KW, Baskin JM, Laughlin ST, Beahm BJ, Naidu NN, Amacher SL, Bertozzi CR. ChemBioChem. 2012; 13:353–357. [PubMed: 22262667]
23. Beahm BJ, Dehnert KW, Derr NL, Kuhn J, Eberhart JK, Spillmann D, Amacher SL, Bertozzi CR. Angew. Chem. Int. Ed. 2014; 53:3347–3352.
24. Salic A, Mitchison TJ. Proc. Natl. Acad. Sci. U.S.A. 2008; 105:2415–2420. [PubMed: 18272492]
25. Li K, Lee LA, Lu X, Wang Q. Biotechniques. 2010; 49:525–527. [PubMed: 20615206]
26. Jao CY, Salic A. Proc. Natl. Acad. Sci. U.S.A. 2008; 105:15779–15784. [PubMed: 18840688]
27. Rieder U, Luedtke NW. Angew. Chem. Int. Ed. 2014; 53:9168–9172.
28. Sasaki E, Kojima H, Hiroaki N, Urano Y, Kikuchi K, Hirata Y, Nagano T. J. Am. Chem. Soc. 2005; 127:3684–3685. [PubMed: 15771488]
29. van Hest JCM, Kiick KL, Tirrell DA. J. Am. Chem. Soc. 2000; 122:1282–1288.
30. Beatty KE, Xie F, Wang Q, Tirrell DA. J. Am. Chem. Soc. 2005; 127:14150–14151. [PubMed: 16218586]

31. Beatty KE, Liu JC, Xie F, Dieterich DC, Schuman EM, Wang Q, Tirrell DA. Angew. Chem. Int. Ed. 2006; 45:7364–7367.
32. Sjoback R, Nygren J, Kubista M. Biopolymers. 1998; 46:445–453. [PubMed: 9838871]
33. Spahn C, Endesflder U, Heilemann M. J. Struct. Biol. 2014; 185:243–249. [PubMed: 24473063]
34. Boens N, Leen V, Dehaen W. Chem. Soc. Rev. 2012; 41:1130–1172. [PubMed: 21796324]
35. Song F, Peng X, Lu E, Wang Y, Zhou W, Fan J. Tetrahedron Lett. 2005; 46:4817–4820.
36. Fahrni CJ, Yang L, VanDerveer DG. J. Am. Chem. Soc. 2003; 125:3799–3812. [PubMed: 12656613]
37. Shie J-J, Liu Y-C, Lee Y-M, Lim C, Fang J-M, Wong C-H. J. Am. Chem. Soc. 2014; 136:9953–9961. [PubMed: 24955871]
38. Koide Y, Urano Y, Hanaoka K, Piao W, Kusakabe M, Saito N, Terai T, Okabe T, Nagano T. J. Am. Chem. Soc. 2012; 134:5029–5031. [PubMed: 22390359]
39. Yogo T, Urano Y, Mizushima A, Sunahara H, Inoue T, Hirose K, Iino M, Kikuchi K, Nagano T. Proc. Natl. Acad. Sci. U.S.A. 2008; 105:28–32. [PubMed: 18172220]
40. Terai T, Urano Y, Izumi S, Kojima H, Nagano T. Chem. Commun. 2012; 48:2840–2842.
41. Kojima H, Nakatsubo N, Kikuchi K, Kawahara S, Kirino Y, Nagoshi H, Hirata Y, Nagano T. Anal. Chem. 1998; 70:2446–2453. [PubMed: 9666719]
42. Kojima H, Hirotani M, Nakatsubo N, Kikuchi K, Urano Y, Higuchi T, Hirata Y, Nagano T. Anal. Chem. 2001; 73:1967–1973. [PubMed: 11354477]
43. Gabe Y, Urano Y, Kikuchi K, Kojima H, Nagano T. J. Am. Chem. Soc. 2004; 126:3357–3367. [PubMed: 15012166]
44. Zhang H-X, Chen J-B, Guo X-F, Wang H, Zhang H-S. Anal. Chem. 2014; 86:3115–3123. [PubMed: 24564742]
45. Romieu A, Massif C, Rihn S, Ulrich G, Ziessel R, Renard P-Y. New J. Chem. 2013; 37:1016–1027.
46. Renier N, Wu Z, Simon DJ, Yang J, Ariel P, Tessier-Lavigne M. Cell. 2014; 159:896–910. [PubMed: 25417164]
47. Uttamapinant C, Tangpeerachaikul A, Grecian S, Clarke S, Singh U, Slade P, Gee KR, Ting AY. Angew. Chem. Int. Ed. 2012; 51:5852–5856.
48. Bevilacqua V, King M, Chaumontet M, Nothisen M, Gabillet S, Buisson D, Puente C, Wagner A, Taran F. Angew. Chem. Int. Ed. 2014; 53:5872–5876.
49. Jiang H, Zheng T, Lopez-Aguilar A, Feng L, Marlow FL, Wu P. Bioconjugate Chem. 2014; 25:698–706.

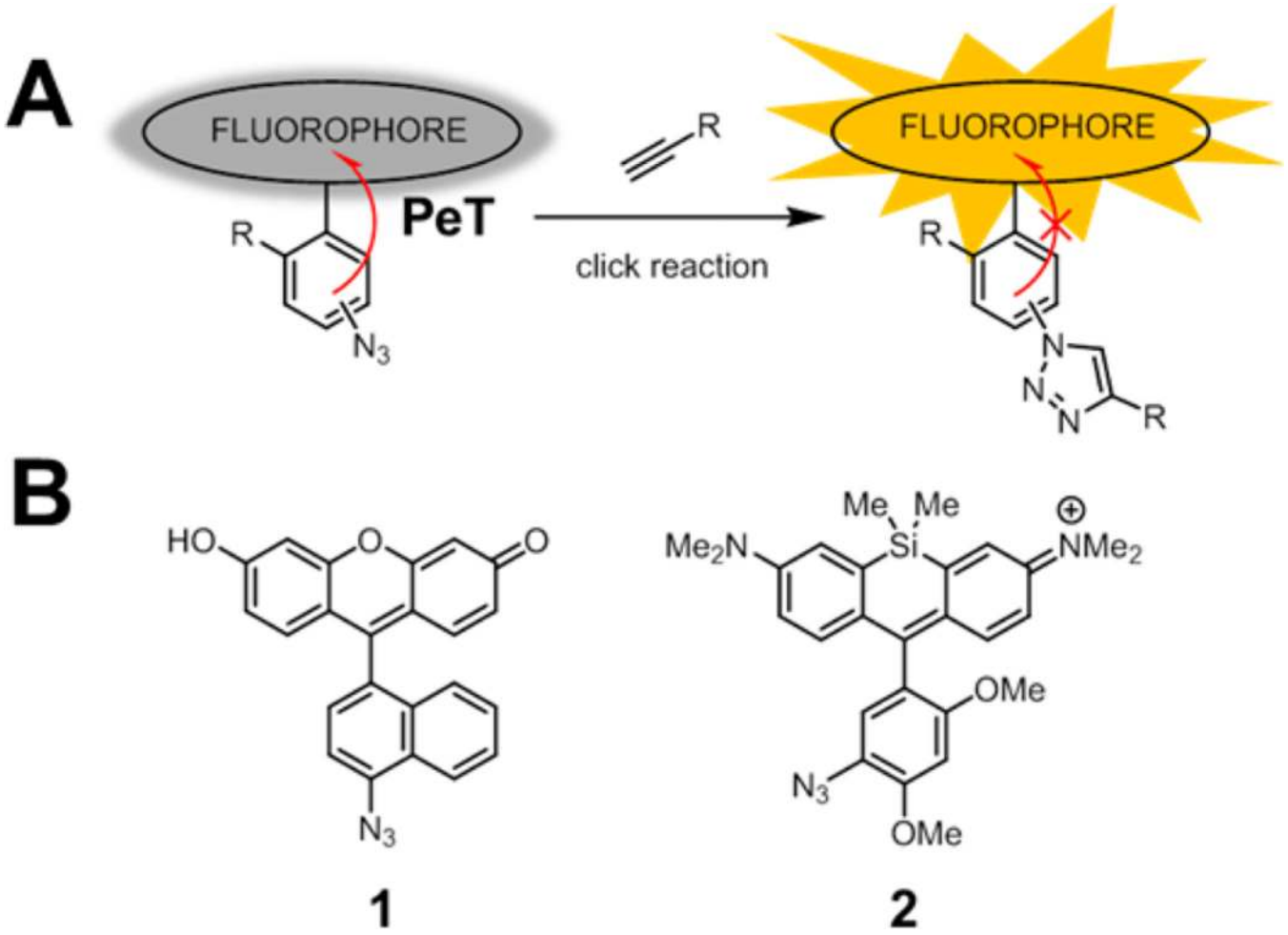


**Figure 1.**

PeT-based fluorogenic azide probes activated by click chemistry. (A) General strategy. (B) Structures of previously described fluorogenic azide probes.

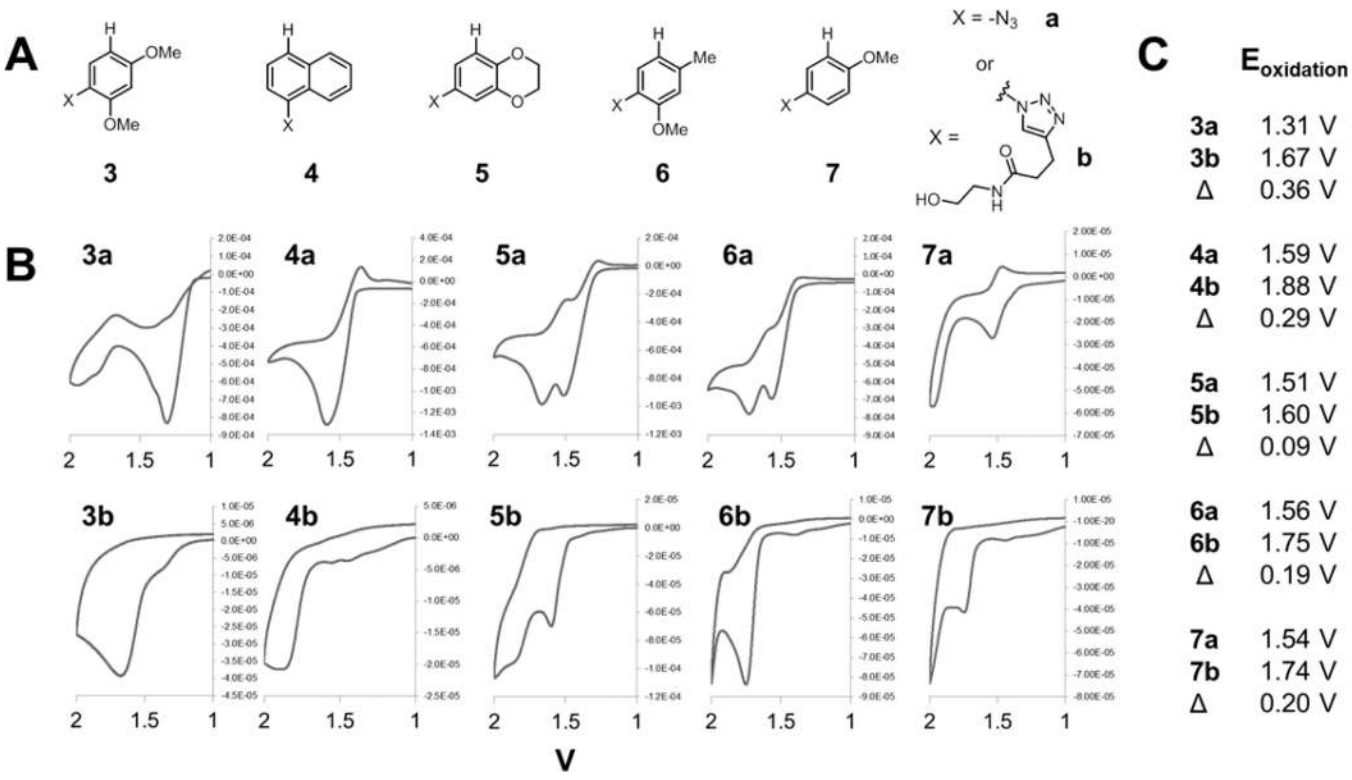


**Figure 2.**

Cyclic voltammetry analysis of substituted aryl systems. (A) Aryl azides (**3a–7a**) and triazoles (**3b–7b**) synthesized and studied by cyclic voltammetry. (B) Cyclic voltammetry plots of compounds **3–7**. (C) Oxidation potentials of compounds **3–7**. Note that all redox cycles were completely or partially irreversible. Cyclic voltammetry was performed in acetonitrile containing 0.1 M $NBu_4PF_6$ as an electrolyte using platinum and glassy carbon electrodes, with a silver reference standard. Ferrocene was added afterward as an internal standard. Scans were performed at 100 mV/s from 0 to 2 V.

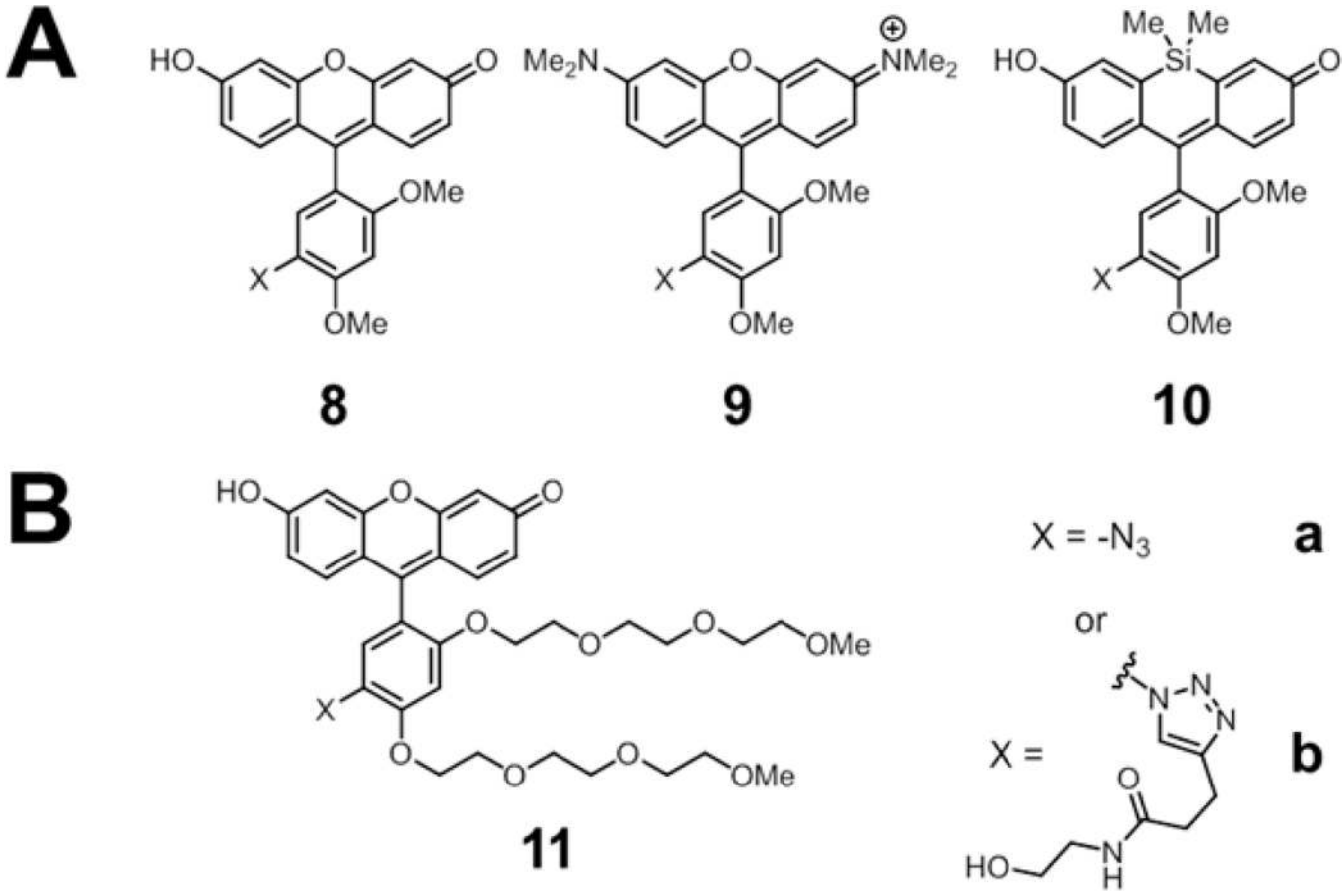


**Figure 3.**

Structures of initial fluorophores prepared in this study. (A) Parent dimethoxy-substituted fluorophores **8–10**. (B) Oligoethyleneglycol-functionalized fluorescein derivative **11**.

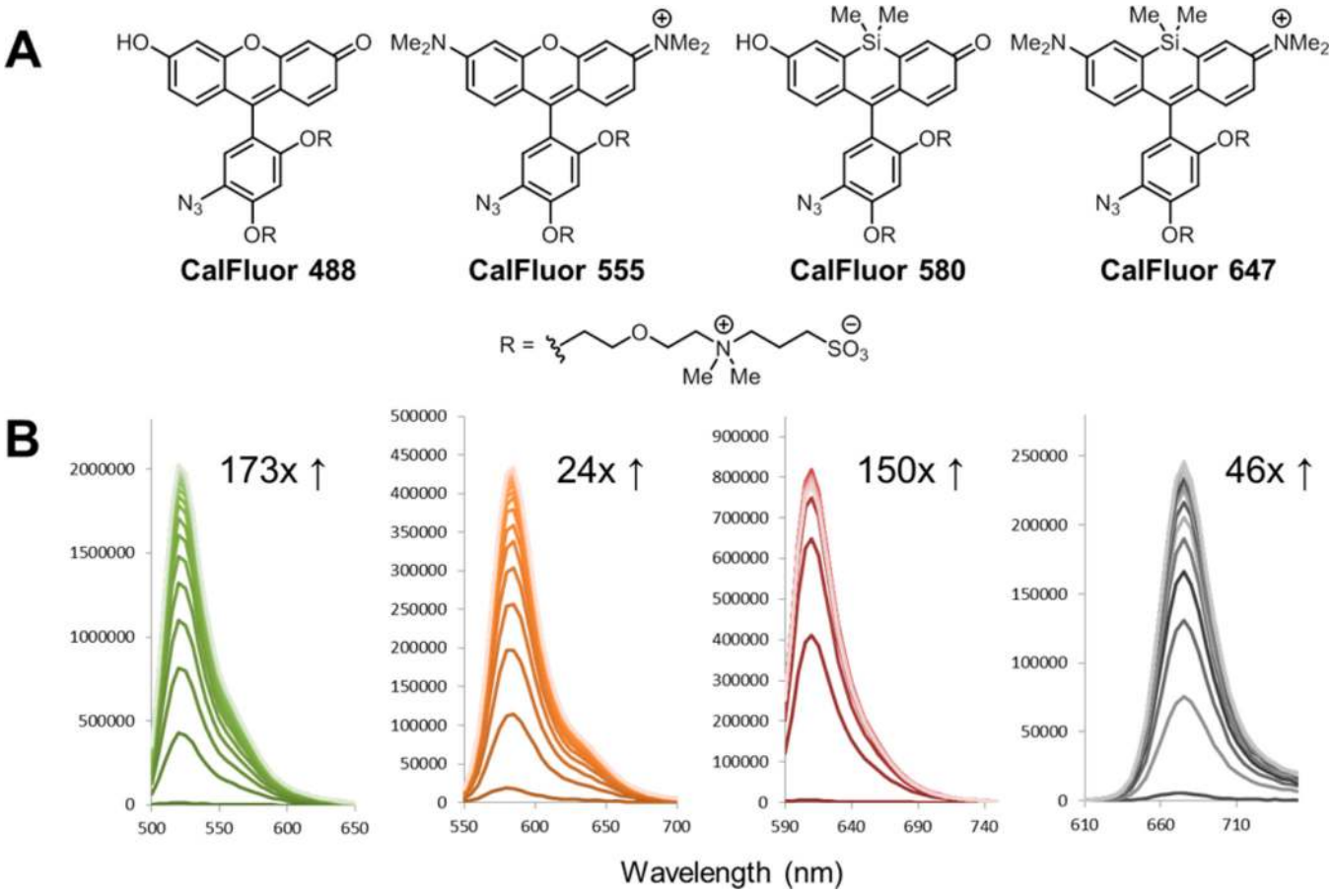


**Figure 4.**

CalFluors and their fluorescence enhancements. (A) Structures of CalFluors 488, 555, 580, and 647. (B) Fluorescence enhancements of CalFluors during copper-catalyzed click reactions. To a mixture of 2 μM fluorophore, 50 μM $CuSO_4$, 300 μM BTTAA ligand, and 2.5 mM sodium ascorbate was added 100 μM alkyne, and emission scans were taken every 30 s. The first scan was taken immediately before addition of alkyne.

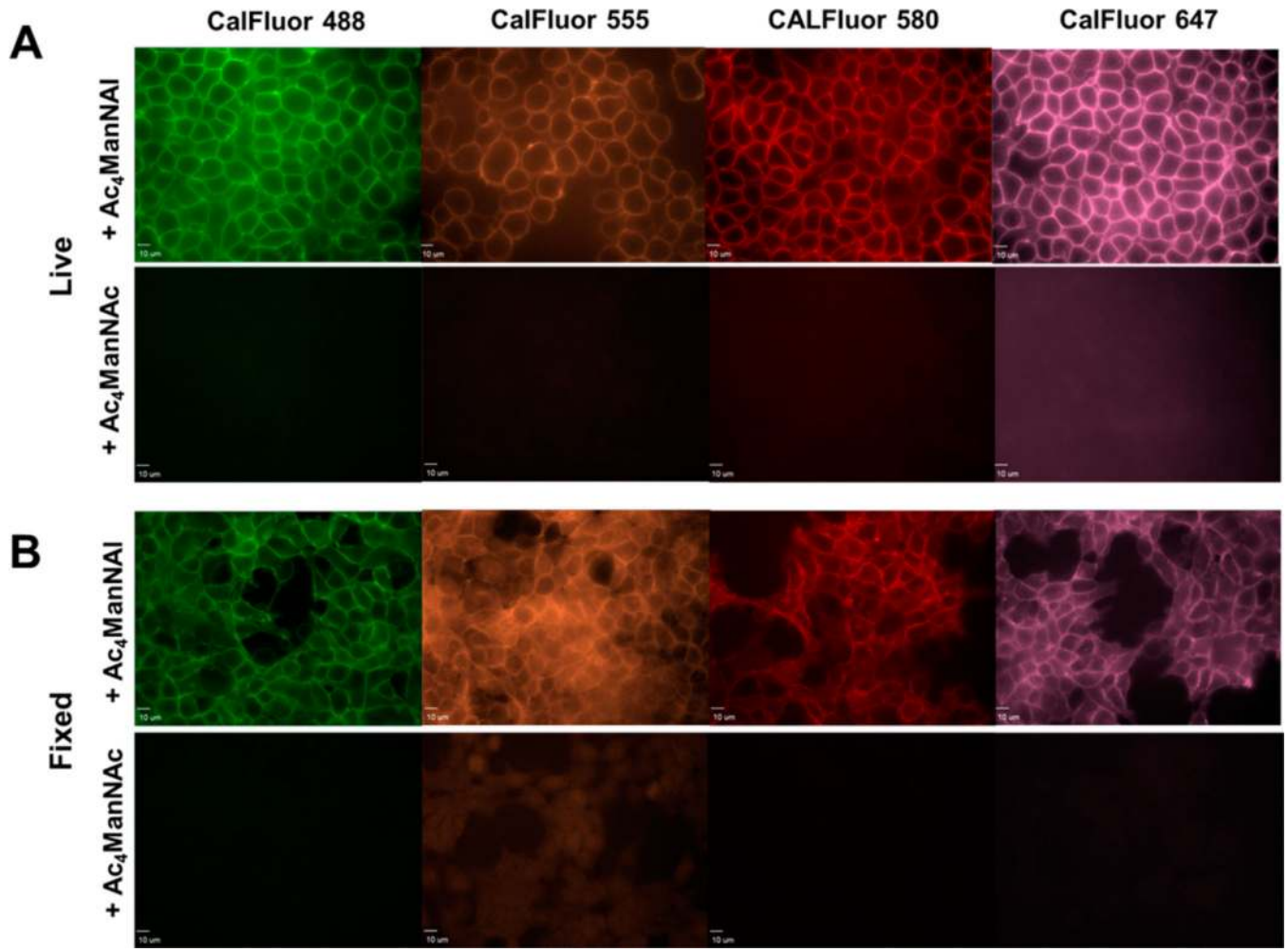


**Figure 5.**

No-wash labeling of cell-surface glycoproteins on HEK 293T cells. Cells were grown with 50 μM $Ac_4$ManNAl or $Ac_4$ManNAc for 3 days and then subjected to click labeling with CalFluor probes. (A) Labeling glycoproteins on live cell surfaces. Cells were treated with 10 μM azide probe, 50 μM $CuSO_4$, 300 μM BTTAA ligand, and 5 mM sodium ascorbate. The reaction was quenched with 1 mM BCS, and the cells were imaged without further wash steps. (B) Labeling glycoproteins on fixed cells. Cells were fixed with 3% paraformaldehyde and then treated with 10 μM CalFluor probe, 1 mM $CuSO_4$, 100 μM TBTA ligand, and 2 mM sodium ascorbate. 0.1 mg/mL BSA was added to prevent the TBTA from precipitating over the course of the reaction. Scale bar = 10 μm.

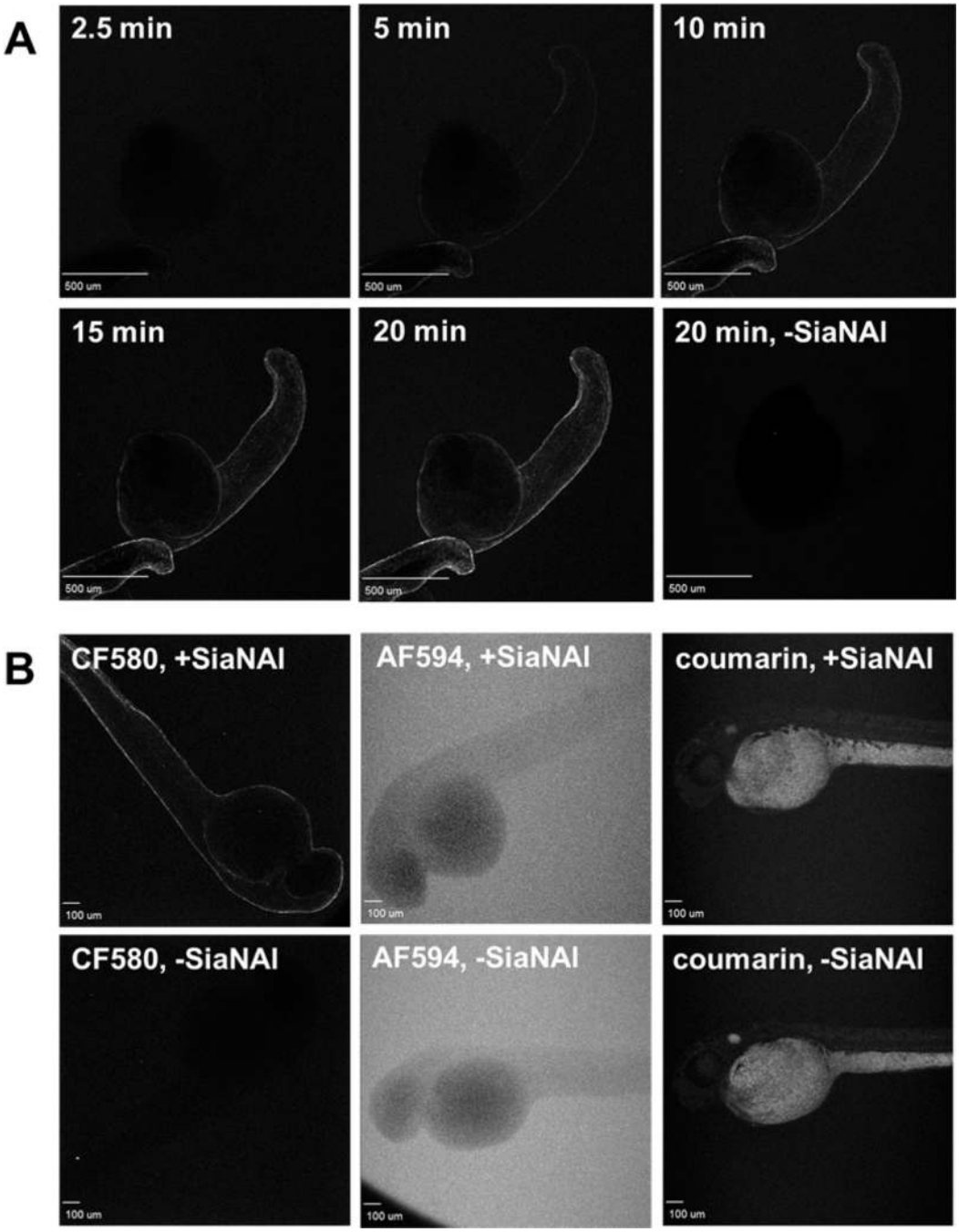


**Figure 6.**

Visualizing sialic acids on live developing zebrafish with CalFluors. Zebrafish were injected with 50 pmol SiaNAl at the one- to four-cell stage and allowed to develop over time. (A) Real-time labeling of sialic acids. After 24 hpf, zebrafish were incubated in a solution containing 1 μM CalFluor 580 and copper catalyst. Alkynedependent labeling was observable after 5 min, and appeared to saturate at 20 min. Scale bar = 500 μm. (B) Comparing no-wash labeling performance by azide probes. After 36 hpf, the embryos were transferred to a solution containing the fluorophore (1 μM for CalFluor 580 and AlexaFluor

594 alkyl azide, or 5 μM for 3-azido-7-hydroxycoumarin) and copper catalyst and imaged without washing after 20 min. Only zebrafish labeled with CalFluor 580 show alkynedependent fluorescence signal. Scale bar = 100 μm.

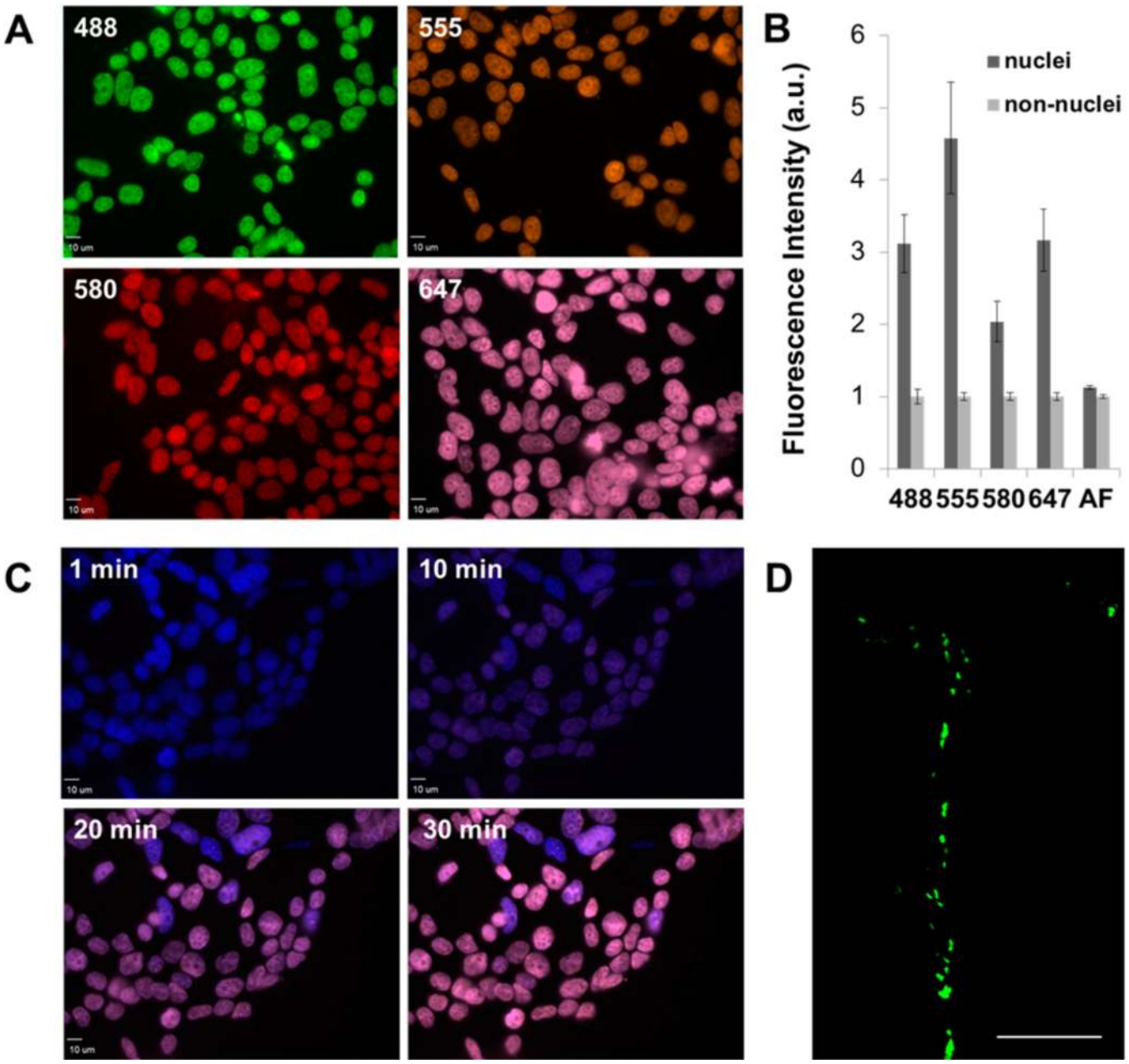


**Figure 7.**

Visualizing EdU-labeled DNA in fixed and permeabilized samples using fluorogenic azide probes. (A) No-wash labeling of EdUlabeled HEK 293T cells. Cells were treated with EdU for 16 h, fixed and permeabilized, and then treated with 10 μM CalFluor probe, 1 mM $CuSO_4$, 100 μM TBTA ligand, 2 mM sodium ascorbate, and 0.1 mg/mL BSA and imaged without further wash steps after 1 h. Scale bar = 10 μm. (B) Quantification of normalized signal over background for the four panels in (A), and comparison to labeling under identical conditions using the non-fluorogenic AlexaFluor 647 alkyl azide (AF). (C) Two-color labeling using Hoescht 33342 and CalFluor 555. After staining with Hoescht, the cells were incubated with a solution of 1 μM CalFluor probe and copper catalyst and imaged in

real-time. Scale bar = 10 μm. (D) Visualization of EdU-labeled newly proliferating cells in mouse brain slices with CalFluor 647. Scale bar = 100 μm.

**Table 1**

Photophysical Properties of All Fluorophores[a]

| compd | $\lambda_{max}$ (nm) | $\lambda_{em}$ (nm) | $\Phi_{fl}$ | enhancement |
|---|---|---|---|---|
| **8a** | 497 | 516 | 0.0059 | – |
| **8b** | 498 | 520 | 0.437 | 74× |
| **9a** | 555 | 577 | 0.0178 | – |
| **9b** | 557 | 580 | 0.351 | 20× |
| **10a** | 586 | 604 | 0.00136 | – |
| **10b** | 588 | 604 | 0.240 | 176× |
| **2** | 654[b] | 666[b] | 0.0042[b] | – |
| **2 triazole** | 665[b] | 668[b] | 0.20[b] | 48×[b] |
| **11a** | 499 | 519 | 0.00589 | – |
| **11b** | 499 | 520 | 0.743 | 126× |
| CalFluor 488 | 498 | 520 | 0.00306 | – |
| CalFluor 488 triazole | 500 | 521 | 0.0747 | 243× |
| CalFluor 555 | 557 | 577 | 0.0174 | – |
| CalFluor 555 triazole | 561 | 583 | 0.604 | 35× |
| CalFluor 580 | 588 | 611 | 0.00250 | – |
| CalFluor 580 triazole | 591 | 609 | 0.473 | 189× |
| CalFluor 647 | 655 | 678 | 0.0056 | – |
| CalFluor 647 triazole | 657 | 674 | 0.25 | 45× |

[a] Measurements were made in pH 7.4 phosphate-buffered saline.

[b] Data from ref 4.